ISOCAM PHOTOMETRY

J. A. D. L. Blommaert[1], K. Okumura[2] and F. Boulanger[2]

[1]ISO Data Centre, European Space Agency, Villafranca del Castillo, P.O. Box 50727, 28080 Madrid, Spain
[2]Institut d'Astrophysique Spatiale, Université Paris XI, 91405 Orsay

ABSTRACT

An overview is given of the flux calibration of the ISOCAM filters and CVF, which was based on observations of standard stars. Observations of non-stellar sources like asteroids and the zodiacal background are used to test the calibration. The ISOCAM responsivity was very stable throughout the ISO mission. There is however a trend of decreasing responsivity for LW by about 6% from start to end within the orbit. Finally some important aspects for deriving photometry on ISOCAM images are discussed.

Key words: ISO – Photometry

1. THE CALIBRATION STARS

The absolute flux calibration of the ISOCAM instrument (Césarsky et al. 1996) is based on observations of standard stars, which are the most reliable calibration sources in the $2-18\mu m$ ISOCAM wavelength range. Before and during the ISO operations, Spectral Energy Distributions (SED) were provided by Cohen et al. (1996 and these proceedings) and by the so-called Ground Based Preparatory Programme (GBPP, Hammersley et al. 1998 and also these proceedings). Later, new SEDs were provided by Decin who, through an iterative process using SWS data, produced a set of theoretical spectra (Decin 2003).

For the calibration of the ISOCAM *fixed filters* the selection of stars was mainly based on the list of calibration stars provided by the GBPP. The overall SEDs (Kurucz models fitted to visible and near-infrared data) are believed to be correct within 5%. The flux densities of the selected sources at 4.5 and 12 μm show quite a variety in flux levels (from 10mJy up to more than 10Jy). Because of the required high visibility throughout the mission all sources are situated in a relatively small region of the sky which has an almost 100% ISO visibility (R.A. $\approx$ 16 hrs, DEC $\approx$ 55^o). In the selection of the stars it was also required that a star be observed at least three times in the near-infrared in the GBPP. The stars were checked not to have any sign of variability nor to be part of a multiple system. As the ISOCAM instrument was quite sensitive it was important to select sources which would not saturate the detectors. This meant that "better known" standard stars, which were used by other instruments were often not usable for ISOCAM. In order to allow cross-calibration some of those stars were observed in the few filters which did not saturate the camera. In total fifteen stars were observed to calibrate the ISOCAM filter responsivities (for the list of stars and a further description see Blommaert et al. 2000 or Blommaert 1998).

Care has to be taken at some wavelengths where the stars may show spectral features: this is especially true for later type stars. Examples of this in the ISOCAM wavelength range are the CO bands between 4 and 5 μm and the SiO fundamental around 8 μm. The Kurucz model does not have any correction for the SiO fundamental. Basically there are ways to try to correct for the different spectral features: for instance by using the Cohen "composite spectra" (Cohen et al. 1996), but these stars were rather bright for ISOCAM so that we selected mainly stars of early spectral type (A, F and G). We believe that this set of stars gives us a very reliable set of absolute flux calibrators.

For the calibration of the ISOCAM *Circular Variable Filters (CVF)*, brighter stars could be selected and here we included stars like γ Dra, δ Dra and Sirius, which were also observed by other instruments. We used the models provided by Decin up to 12 μm and Cohen at longer wavelengths. The differences between the 2 input SEDs are discussed by Decin 2003. In the wavelength ranges we observed the differences were only at the percent level. A more detailed description can be found in the ISOCAM CVF photometry report (Blommaert et al. 2001a).

In section 4 we will discuss the observations of non-stellar objects which were used to verify the flux calibration of the instrument.

2. ABSOLUTE FLUX CALIBRATION

The flux calibration observations were done in staring mode with the source at the centre of the arrays. The data-analysis of the standard star measurements was performed within the CIA (CAM Interactive Analysis, Ott et al. 1996) package and followed a standard procedure, including: deglitching (method= 'temp'), averaging the frames on the stabilised part, flat-field correction and background subtraction.

The conversion of the measured signal in ADU/G/s to a flux density F_ν in Jy is given by the SENSITIV parameter in the CCG*WSPEC calibration files (see the ISO Handbook Vol. III: CAM, Blommaert et al. 2001b). The SENSITIV parameter is given for the so-called reference wavelength of each filter. The absolute flux calibration of ISOCAM follows that adopted for IRAS. The convention used is that the conversion from mea-

Proceedings of the Conference "The Calibration Legacy of the ISO Mission", VilSpa, Spain, February 2001
ESA SP-481, 2003, eds. L. Metcalfe, A. Salama, S. B. Peschke & M. F. Kessler

sured signal (ADU/G/s) to Jy is given for a $\lambda F_\lambda(\lambda) = const.$ spectrum. For a source with a different spectrum a colour correction has to be applied.

2.1. The LW detector

The comparison of signal per flux density of the measured stars shows a scatter of typically 5% RMS. This scatter contains the uncertainty in the stellar models, the uncertainty in the stabilisation of the signal (section 6) and the fact that different configurations were used to observe the stars (see subsection 2.3). Fig. 1 shows the comparison of pre-launch and in-orbit determined values. The new LW values are close to the pre-launch ones.

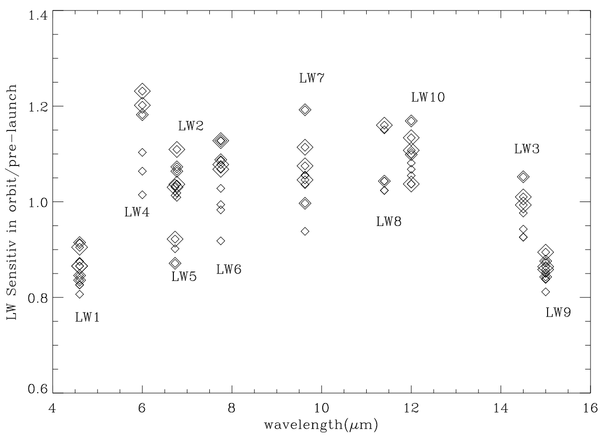

Figure 1. The in-orbit LW SENSITIV values compared to the pre-launch values. 1.5, 3 and 6″ PFOV measurements are included. The smallest symbols are 1.5″ and the largest are 6″ measurements.

2.2. The SW detector

For SW the results of the photometric observations and the comparison with the ISOCAM 'pre-launch' can be seen in Fig. 2. For most filters the RMS is rather small (less than $\sim 5\%$). There is a clear decrease in the difference with the ground-based SENSITIV values and the ones observed in orbit with increasing wavelength. The reason is that in the routine determining the pre-launch values given in the ISOCAM manual a 'λ-factor' was missing (private communication, M. Pérault). The ratio between the ground-based and in orbit SENSITIV values for the SW filters is similar to the one found for the Spectral Response Functions measured pre-launch and in orbit (Biviano et al. 1998).

2.3. Different Configurations

Measurements on calibration stars were also performed to investigate possible dependencies on different configurations. Different readout times were used and showed no significant

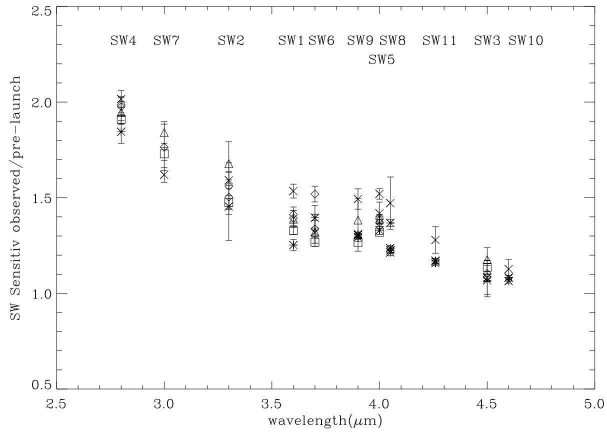

Figure 2. The in-orbit SW SENSITIV values compared to the pre-launch values. 1.5, 3 and 6″ PFOV measurements are included. The different symbols correspond to different stars used. (See the text for an explanation of the gradient.)

differences. Also for different pixel fields of view (PFOV): 1.5, 3 and 6″, only small and no systematic differences could be found. There is however some tendency that the 1.5″ PFOV leads to somewhat weaker signals (Blommaert et al. 2000, Blommaert 1998).

3. CVF SPECTRAL RESPONSE FUNCTION

As was mentioned in Sect 1, the SRF is determined from calibration star observations. This strategy followed the one used for the filter photometric calibration. In brightness range the stars span 2 orders of magnitude. In comparison to the ones selected for the filter calibration, they are relatively bright because the band width on a segment of CVF is small compared to those of the large bandpass filters.

In contrast to the filter measurements stabilisation plays a less important role as the signal changes are smaller between different CVF steps. The most crucial part in this respect is the start of the measurement where the signal step is most likely the largest one. This effect was minimised by starting the measurement at the short wavelength side where the flux of the star is the highest and the signal stabilises fastest. The effect of the stabilisation was checked with back- and forward scans. The main difficulty for photometry with the CVF is the presence of reflected light on the detector configuration which falls in part back on the point source itself (Okumura et al. 1998). To avoid this contribution we first tried psf-fitting, but as the theoretical PSF and the CVF observed one do not match well enough, deviations were found in the photometry. We used aperture photometry, taking special care to avoid the ghost (Blommaert et al. 2001a). In order to minimise the photometric error on any ISOCAM astronomical CVF data, it is recommended to use, as close as possible, the same photometry method as that adopted for the calibration measurement. Aperture radii of 6, 4, 3 pixels for 1.5, 3 and 6″ PFOV respectively were used. The background was taken in an annulus 2 pixels wide.

The resulting SRF available in the calibration file is determined on the basis of the measurements of the different stars. The different measurements give a typical RMS of 3-4% for both detectors (see Figures 3 and 4). The spread is caused by the use of different sources and the use of different optical configurations. The latter leads to differences in the stabilisation and the necessity to use different apertures. Larger PFOVs lead to slightly higher total signals (Blommaert et al. 2001a).

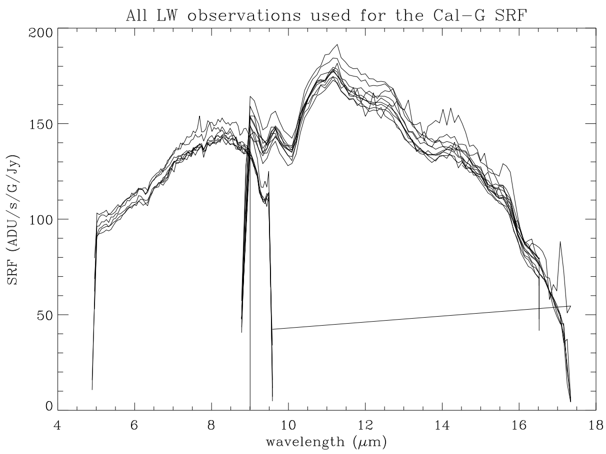

Figure 3. The different SRF determinations based on the observations of 4 different calibration stars. It includes different PFOV measurements. The RMS is 3-4 %.

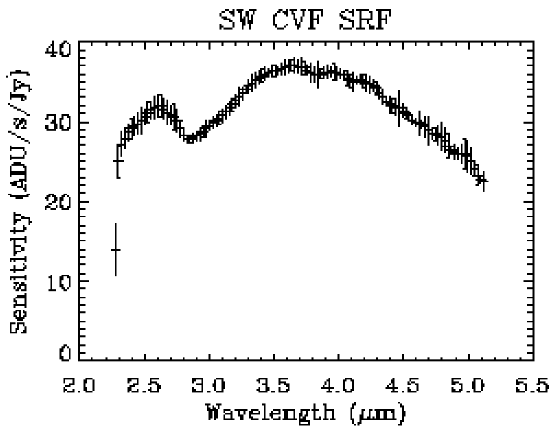

Figure 4. The SW SRF within its $\pm 1\sigma$ confidence band (Biviano et al. 1998).

4. NON-STELLAR CALIBRATION SOURCES

Some objects with SEDs very different from stars were also observed to check independently the flux calibration and the colour corrections. They also provided a comparison between the CVF and the filters.

4.1. POINT SOURCES

Not many non-stellar point sources are well modelled and we observed with both the CVF and filters to be able to calibrate them. We selected very red objects like asteroids and dust-shell obscured AGB-stars. A good agreement was found between the CVF and the (colour corrected) filter measurements, showing that the colour corrections were accurate up to the precision of our point source photometry (a few percent).

4.2. EXTENDED EMISSION

The validity for extended sources of the ISOCAM stellar calibration was tested on observations of high latitude sky areas where, at mid-IR wavelengths, the Galactic emission is negligible with respect to the zodiacal light (Galactic/zodiacal emission $\sim 1\%$). For these observations, the sky brightness is uniform within the $3'$ field of view and one can compare the ISOCAM brightness with DIRBE related predictions of the zodiacal sky brightness at the position and time of the observations. We have done this for a significant set of filter and CVF observations. For a given observation, one ISOCAM brightness is computed from the mean flux over the non-vignetted part of the camera divided by the pixel area in ADU/G/s/sr and converted into Jy/sr with the SRF obtained with stellar observations as described in Sect. 3. The zodiacal light flux estimates were derived from the model of Kelsall et al. 1998. These model parameters were fitted in order to reproduce the DIRBE broadband measurement of the zodiacal light including three mid-IR wavelengths 4.9, 12 and $25\mu m$. Its accuracy at these wavelengths, within the range of solar elongations used by both ISO and DIRBE, is estimated to be of the order of a few percent. The details of the spectral dependence of the zodiacal light, in particular the plausible existence of silicate emission bands, are poorly constrained by the DIRBE data. The Kelsall et al. 1998 model is thus based on simple assumptions about the emissivity of interplanetary dust which can be tested by ISOCAM observations.

Fig. 5 shows the mean ratio between ISOCAM fluxes and the Kelsall et al. 1998 model for diverse ISOCAM filters and pixel fields of view. All data points are scattered within 10% of 1, except one short–wavelength point which is noisy (dark uncertainties become important with respect to expected zodiacal light brightness at the shortest ISOCAM wavelengths) and three points with the 12” PFOV which are slightly above 1.1. This good agreement for filter observations between ISOCAM and DIRBE zodiacal fluxes is quite satisfactory. Uncertainties in the spectral dependence of the zodiacal emission, in the ISOCAM calibration and in the photometric accuracy of ISOCAM measurements (limitations in our understanding of long term gain variations with illumination) can all contribute to the observed scatter and it is difficult to disentangle the respective contributions.

The results for the CVF observations (Fig. 6) are less satisfactory than for the filters due to multiple reflections between the ISOCAM detector and CVF. The CVF ISOCAM images of the zodiacal light obtained after flat-field corrections are not flat: they present two "lung-shaped" bumps to the left and right sides of the detector. The reflections not only distort the image, they also affect the calibration by bringing additional flux onto the detector. In the stellar calibration we were careful in separating spatially the ghosts from the main image. Since this spatial separation is obviously not possible for extended sources, the additional flux brought by the reflections is included in the zodiacal brightness measurement but excluded in the stellar calibration of ISOCAM. This explains why the two curves in Fig. 6 are systematically above 1. This figure also shows that the amplitude of this effect for extended source calibration varies significantly with wavelength and thus affects not only the overall flux calibration but also the shape of the spectra. The CVF stellar observations permit correction for this spectral dependence of the reflected light under the assumption that it is independent of the source position. We have used observations where the ghost was well displaced from the main star image to estimate the spectral dependence of its relative amplitude (See Blommaert et al. 2001a for more details). Fig. 7 shows the CVF to zodiacal model ratio after correction by this determination of the stellar ghost amplitude. This correction brings the CVF into agreement with the filter data points. This is a quite satisfactory result which gives us confidence in the assumption made in extrapolating the measurement at one source position to the whole camera field of view. The spectral dependence left in the CVF data could represent a real spectral dependence of the zodiacal emission not taken into account in the Kelsall et al. 1998 model.

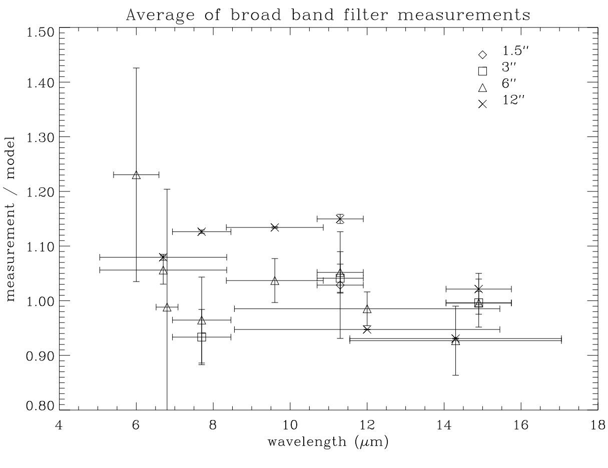

Figure 5. Mean ratio between ISOCAM and DIRBE zodiacal light model for filter observations in regions of low Galactic emission. Each data point represents the mean value of a number (ranging from 1 to a few) of observations for a given pfov and filter combination. The horizontal bars indicate the band widths of the filters. The vertical error bars indicate the standard deviation (which is larger than the RMS of the mean value).

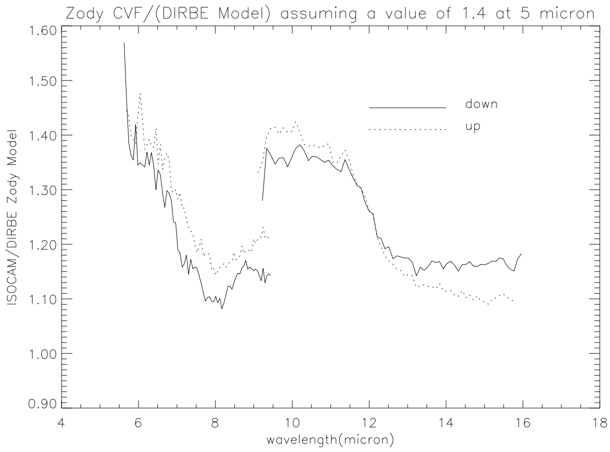

Figure 6. Mean ratio between CVF spectra and DIRBE zodiacal light model computed over a set of 14 observations performed both down and up in wavelengths. The two curves do not match perfectly. The difference is the residual effect of the gain variations left after Fouks-Schubert transient correction.

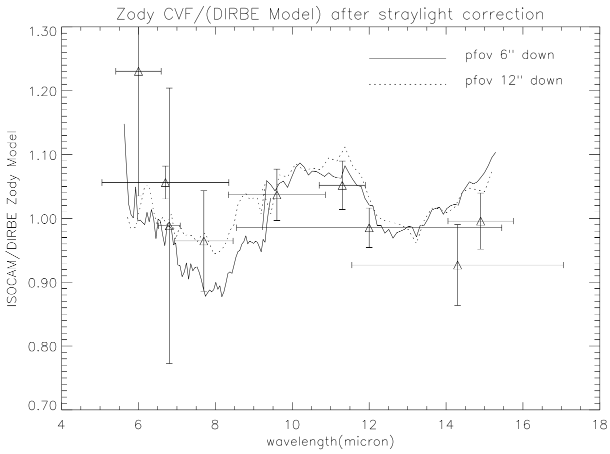

Figure 7. Ghost corrected CVF zodiacal light measurement normalised to the zodiacal light model. Also shown are the broad band filter, 6″ PFOV measurements with error bars. The horizontal bars indicate the filter band widths.

5. RESPONSIVITY TREND

HIC89474 (=HR6847) was regularly observed to monitor the responsivity throughout the mission. Measurements were done with the 2 detectors. The source has also been observed to check for variation throughout the orbit. For the LW detector, a trend of decreasing responsivity with time since activation was found with a difference of about 6% between the beginning and end of the revolution. When correcting the photometry throughout the mission for this in-orbit dependence we find that the LW response has remained stable throughout the mission and that the overall scatter has a two percent RMS.

SW also only showed a small variation throughout the mission (RMS= 2%) and no significant trend is found. Nor was there any significant trend found as a function of time in orbit. (See also **??** for the trend analysis with the internal calibration devices).

6. IMPORTANT POINTS FOR CAM PHOTOMETRY

Here we want to discuss two important aspects when deriving photometry on ISOCAM images.

6.1. PSF-Correction

In order to derive photometry consistently for point sources observed under different conditions and to have the absolute flux calibration also applicable on extended sources, the point source flux is determined by using aperture-photometry and scaling the resultant flux for the part of the PSF which was not included in the aperture. The correction for the missing part of the PSF is an important one as the PSF's can be very large, especially at the longest wavelengths and for a PFOV of $1.5''$. For an aperture of approximately 6 times the Airy disk FWHM ($6 \times \lambda(\mu m)/3$, Blommaert et al. 2001b) the correction can be up to 20%.

A warning has to be given that the theoretical PSF is not a perfect representation of the observed one and that the corrections applied when using small apertures are underestimated (Blommaert et al. 2001a).

As was mentioned in section 3 the ghost contribution in the CVF complicates the aperture photometry. We recommend to use the same apertures as applied for the calibration of the SRF: radii of 6, 4, 3 pixels for 1.5, 3 and $6''$ PFOV respectively and a background determination in an annulus 2 pixels wide.

6.2. Stabilisation

A dominant uncertainty in the photometry is the way the signal stabilises after each flux step. The transient behaviour of the detector is dependent on the flux step and can take very long for weak fluxes. For LW the transient has two components: a short-term one which affects 40% of the flux step and a long-term one which affects 5-10%. The latter one is little understood and is only reached in very long measurements. The flux calibration is based on stabilised signals after the short-term trend (Coulais & Abergel 2000). SW shows another behaviour with only a monotonic change.

CIA offers routines that select the part of the data which is assumed to be stabilised. This, of course, works well only when the final signal value has indeed been reached (for instance with bright sources). In cases where the signal has not reached stabilisation one needs to apply other routines that fit a transient model to the data and then correct for it. The method applied in the ISOCAM Off Line Processing is called the Fouks-Schubert method (Coulais & Abergel 2000) which is currently capable of giving photometric results for extended emission within a few percent. The correction is not meant for point sources but in most cases improves the data. For a discussion on the particular transient behaviour of point sources see Coulais & Fouks 2003 In the case of the photometry of standard stars, which are relatively bright, the signal is relatively well stabilised by the end of the 200-seconds measurement.

REFERENCES

Biviano, A., Altieri, B., Blommaert, J. et al., 1998, The ISOCAM CVF Calibration Report, http://www.iso.vilspa.esa.es/
Blommaert, J.A.D.L., 1998, ISOCAM Photometry Report, http://www.iso.vilspa.esa.es/
Blommaert, J.A.D.L., Metcalfe, L., Altieri, B. et al., 2000, Experimental Astronomy 10, 241
Blommaert, J.A.D.L., Boulanger, F., Okumura, K., 2001a, ISOCAM CVF photometry report, ESA technical report
Blommaert, J.A.D.L. et al., 2001b, ISO Handbook Vol. III: CAM - The ISO Camera, SAI/99-057/Doc
Cohen, M. et al., 1996, AJ 112, 2274
Césarsky, C., Abergel, A., Agnèse, P. et al., 1996, A&A 315, L32
Coulais, A., Abergel, A., 2000, A&AS 141, 533
Coulais, A., Fouks, B., 2003, this volume
Decin, L., 2003, this volume
Gallais, P., 2003, this volume
Hammersley, P. et al., 1998, A&AS 128, 207
Hammersley, P., Jourdain de Muizon, M., 2003, this volume
Kelsall, T. et al., 1998, ApJ 508, 44
Okumura, K., Pérault, M. and Longval, Y., 1998, Ghosts in ISOCAM images, Technical report, http://www.iso.vilspa.esa.es/